Supplementary Material (ESI) for Lab on a Chip

Electronic Supplementary Information (ESI)

For the Manuscript

Traction Force Microscopy On-Chip: Shear Deformation of Fibroblast Cells

Tamal Das,[a] Tapas K. Maiti,[a] Suman Chakraborty[b,1]

[a] Department of Biotechnology, Indian Institute of Technology, Kharagpur – 721302, India

[b] Department of Mechanical Engineering, Indian Institute of Technology, Kharagpur – 721302, India

[1] Corresponding Author, Email: suman@mech.iitkgp.ernet.in

Detailed Description of the Physical Model and Simulation

1. Expression for velocity field

In the limit of low Reynolds numbers typical to microchannel flows, the linear superposition theorem holds valid [1] and accordingly, the velocity field at any point can be composed of the following components: (i) velocity of the unperturbed background Poiseuilli flow ($\mathbf{v}_1$), (ii) perturbation to the velocity due to the force applied by the vesicle on the fluid ($\mathbf{v}_2$), and (iii) perturbation to the velocity due to the force applied by the substrate on the fluid ($\mathbf{v}_3$). A complete summation expression for velocity $\mathbf{v}(\mathbf{r},t)$ can accordingly be described as: [2]

$$\mathbf{v}(\mathbf{r},t) = \mathbf{v}_1 + \int_{\Gamma_v} \mathbf{G}(\mathbf{r}-\mathbf{r}')\mathbf{f}_{\text{memb}}(\mathbf{r}')d\mathbf{s}' + \int_{\Gamma_s} \mathbf{G}(\mathbf{r}-\mathbf{x}')\mathbf{f}_{\text{subs}}(\mathbf{x}')d\mathbf{x}' \quad (1)$$

while the imposed pressure driven flow is described as

$$v_{1,x}(y) = \frac{-dp/dx}{2\mu} y(H-y) \quad \text{and} \quad v_{1,y} = 0 \quad (1a)$$

Here, dp/dx is the imposed pressure gradient, H is the height of microchannel, and μ is the viscosity of the fluid. Vesicle and substrate boundaries are represented by Γ_v and Γ_s. The tensor $\mathbf{G}$ in this expression is the Green's tensor for free space and is derived as

$$G_{ij} = \frac{1}{4\pi\mu}(-\delta_{ij}\ln r + \frac{r_i r_j}{r^2}) \quad (2)$$

where r_i is the i^{th} component of the vector $\vec{r}-\vec{r}'$ and δ_{ij} is the Kronecker delta. Based on the flow-filed described as above, one may derive pertinent expressions for the membrane force, f_{memb}, and the substrate force, f_{subs}, as detailed subsequently.

1.1. Derivation of Membrane Force

An expression for f_{memb} may be derived on the basis of curvature energy, adhesion energy and the conservation of local length scale. The force component due to the membrane curvature, which is derived as functional derivative of Helfrich curvature energy, is expressed as

$$f_{curv} = \kappa(\frac{\partial^2 c}{\partial s^2} + \frac{c^3}{2})\hat{n} \tag{3}$$

where $\kappa, c, \hat{n}$ are the bending rigidity, local curvature, and the unit normal vector, respectively. Analogously, the adhesion force component is written as

$$f_{adh} = -(cw(r) + \frac{\partial w(r)}{\partial n})\hat{n} \tag{4}$$

The short range adhesion potential $w(r)$ accounts for the membrane-substrate interaction and is approximated by a spring model possessing equilibrium length l_0 and a spring constant k_{adh}, as follows:

$$\nabla w(r(x,y)) = k_{adh}(l - l_0)[(\frac{x - x_{p,subs}}{l})\hat{x} + (\frac{y - y_{p,subs}}{l})\hat{y}] \qquad \text{for } l < l_{crit}$$

$$= 0 \qquad \text{for } l \geq l_{crit} \tag{5}$$

Here $x_{p,subs}$ and $y_{p,subs}$ are the coordinates of the corresponding point where the substrate-end of the adhesion spring is attached and l_{crit} is the critical length of the spring beyond which the adhesion is considered to be snagged off. From previous theoretical and experimental reports,[3-5] l_{crit} is taken to be 1.1 times of the equilibrium length (l_0) whereas the value of k_{adh} is taken as 10^{-3} (N/m) per μm^2 assuming there are approximately 1000 adhesion sites per μm^2 which is fairly standard. [6] The third component of the membrane force arises from the conservation of local membrane length. Biologically, the membrane is composed of insoluble amphiphilic phospholipids bi-layer with proteins embedded in it and is assumed to be an incompressible fluid in two-dimensional spaces.[2] This fact promptly points towards the incompressibility of local arc-length. In order to impose this constraint, a local Lagrange multiplier $\zeta(s)$ is introduced and on subsequent differentiation to energy functional associated with it, the resultant expression for the relevant force yields

$$f_l = \frac{\partial \zeta}{\partial s}\hat{t} - c\zeta\hat{n} \tag{6}$$

where $\hat{t}$ is unit vector in tangential direction. Combining equations (3), (4) and (6), the net expression for f_{memb} is obtained as

$$f_{memb} = \kappa(\frac{\partial^2 c}{\partial s^2} + \frac{c^3}{2})\hat{n} - (cw(r) + \frac{\partial w(r)}{\partial n})\hat{n} + \frac{\partial \zeta}{\partial s}\hat{t} - c\zeta\hat{n} \quad (7)$$

1.2. Substrate Force

Utilizing the definition of the stress tensor $\sigma_{ij} = -p\delta_{ij} + \mu(\frac{\partial v_i}{\partial x_j} + \frac{\partial v_j}{\partial x_i})$, the substrate force per unit area can be obtained as

$$f_{subs} = p\hat{y} - \mu\frac{\partial v_x}{\partial y}\hat{x} \quad (8)$$

2. Model Simulation

2.1. Numerical Implementation

The cell membrane is discretized in 200 points, considering equal arc lengths between each neighboring pair. Similarly, substrate underneath the cell is also discretized in 200 points. However, while the distance between neighboring substrate points close to the cell is kept fixed at 50 nm, it is exponentially increased for the points away from the cell owing to their decreasing effects on the velocity field in the cell's proximity. Starting from an initial condition, the grid points are moved by a distance $v_n dt$ in normal direction after each timestep. Following the works by Cantat *et al*,[2] the numerical scheme is broadly classified into three major steps, namely, (i) determination of the membrane force ($f_{memb,i}$) at each point on the membrane using equation (7), (ii) estimation of the wall reaction force assuming a non-slip condition at the wall, which provides the numerical values of p, $\partial v_x/\partial y$ and subsequently f_{subs} at each grid point on the wall, and (iii) evaluation of the effective velocity at every grid point on membrane by utilizing equation (1). The time step employed for temporal discretization is kept fixed at 10^{-5} s. A major constraint towards implementing this numerical scheme is apparently imposed by the requirements of realization of length and area constraints. From a fundamental perspective, the system demands conservation of both membrane length and the enclosed area simultaneously at any time instant. However, the mutual dependence of the incompressibility equation $v_n c + \partial v_t / \partial s = 0$, the membrane force equation (7) and the

velocity equation (1) imparts an inherent difficulty in explicitly determining the magnitude of the Lagrange multiplier at any timestep. However, the aforementioned criticality may be resolved by employing a 'stiff-spring' like modeling [2] of the Lagrange multiplier, described as follows. Employing an expression: $\zeta = k_{spr}(ds_i - ds_{0,i})$, where ds_i is the instantaneous distance between two adjacent points in the membrane and $ds_{i,0}$ is the reference or initial distance, the length of the membrane is conserved within 0.6%. The magnitude of k_{spr} is set at 10. In similitude, the problem related to the conservation of area is also sorted out by introducing an effective pressure term $p^{eff} = k_{pr}(A - A_0)$, which compels the enclosed area to vary within the 1% of the desired value of A_0. The value of k_{pr} is taken as 10^9. Further details of such numerical considerations are reported elsewhere, [2] and are not repeated here for the sake of brevity. We have also computed cell's centroid displacement in response to a flow velocity. At each time step, co-ordinates of the centroid is computed as $x_c = \sum_{i=1}^{N} x_i / N$ and $y_c = \sum_{i=1}^{N} y_i / N$ where N = 200, x_i and y_i are co-ordinates of membrane points at that time step.

2.2. Equilibrium shape in static condition

As discussed elaborately by Cantat *et al*,[2] the contact length or equivalently the contact area in three dimensions is governed by the membrane rigidity (κ) and mean potential of adhesion ($\overline{w}$). Close to the surface, the membrane curvature smoothly varies from the value obtained in bulk of the cell to zero (please see Fig. 2 in the main text). Thus, at equilibrium, for a cell or vesicle adhering homogeneously to a substrate, the excess membrane energy due to contact curvature (similar to contact angle for a droplet) should be balanced by energy decrease due to the favorable cell-surface interaction. This yields to the equilibrium contact radius of curvature as $R_{eq} = 1/c_{eq} \sim \sqrt{\kappa / 2\overline{w}}$. [2] Hence, one should expect a cell of any arbitrary shape to take its most energetically favorable shape governed by eq. (1) if it is created sufficiently close to the surface, where adhesion force

is effective. However, in order to save computational time, we have geometrically approximated the cell shape in such a way that the following three conditions are satisfied: (i) the cell perimeter is conserved and fixed at a value of $2\pi R$, where R is radius of a cell (~ 5 μm), (ii) the contact angle is fixed at $R_{eq} = \sqrt{\kappa / 2\overline{w}}$, and (iii) the adhesion length is 20% of the total perimeter. Starting with this and maintaining dp/dx = 0; the cells have been found to settle into the equilibrium shape with 50 time iterations. For all shear induced deformation simulations, the value of imposed pressure gradient is set non-zero only after this equilibrium is reached.

3. Theoretical parametric variation of critical shear rate for detachment

In spite of the fact that qualitative concordance between experimental and theoretical findings (please refer to section 4.5 in main text) is satisfied over a large range of values of the pertinent cellular parameters such as viscosity, membrane stiffness, adhesion strength; the exact numerical value of critical shear rate for peeling off has been found to be varying with those parameters (Fig. 1, supplementary information). The standard values of all such sensitive parameters are selected on the basis of previous experimental evidences. [3-6] While the critical shear rate is observed to be higher with increasing adhesion strength and higher viscosity values, this trend is reversed with regard to the stiffness. Biophysical implication of this outcome is extremely significant. It has been found experimentally that shear stress increases the intracellular viscosity by Rho-kinase activation [7] and decreases the membrane rigidity. [8] From the present analysis, it is inferred that these adaptive changes will help in avoiding the cell peel-off by increasing the effective critical shear rate. Thus, the present theoretical modeling is able to capture and forecast cellular adaptation to imparted stress.

.

References

1 I. Cantat and C. Misbah, *Phys. Rev. Lett.*, 1999, **83**, 880-883.

2 I. Cantat, K. Kassner and C. Misbah, *Eur. Phys. J. E*, 2003, **10**, 175-189.

3 S. R. Hodges and O. E. Jensen, *J. Fluid Mech.*, 2002, **460**, 381-409.

4 P. Bongrand, C. Capo and R. Depieds, *Prog. Surf. Sci.*, 1982, **12**, 217-285.

5 G. I. Bell, M. Dembo and P. Bongrand, *Biophys. J.*, 1984, **45**, 1051-1064.

6 A. J. Garćia, F. Huber and D. Boettiger, *J. Biol. Chem.*, 1998, **273**, 10988-10993.

7 J. S. H. Lee, P. Panorchan, C. M. Hale, S. B. Khatau, T. P. Kole, Y. Tseng and D. Wirtz, *J. Cell Sci.*, 2006, **119**, 1760-1768.

8 P. J. Butler, G. Norwich, S. Weinbaum and S. Chien, *Am. J. Physiol. Cell Physiol.*, 2001, **280**, C962-C969.

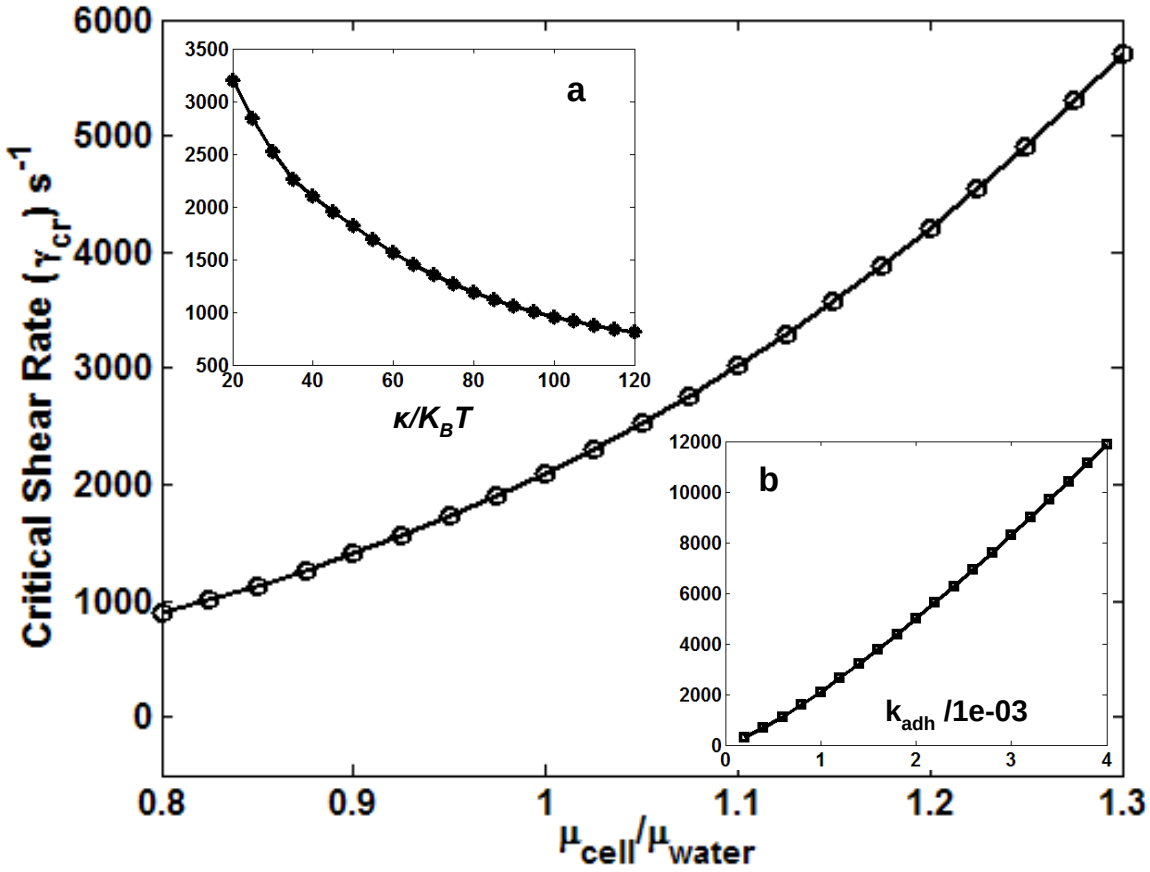

Fig. 1: Variation of critical shear rate ($\dot{\gamma}_{cr}$) with cellular parameters such as – i. viscosity (main image), ii. membrane rigidity (inset a) and iii. strength of adhesion (inset b). For both insets y-axis represents critical shear rate ($\dot{\gamma}_{cr}$).